# ELASTIC WAVE DIFFRACTION BY A SEMI-INFINITE CRACK IN A TRANSVERSELY ISOTROPIC MATERIAL

## By A. N. NORRIS

(Exxon Research & Engineering Corporate Research Laboratory, Clinton, New Jersey 08801, U.S.A.)

## and J. D. ACHENBACH

(The Technological Institute, Northwestern University, Evanston, Illinois 60201, U.S.A.)

[Received 20 June 1983. Revise 6 December 1983]

### SUMMARY

Crack diffraction in a transversely isotropic material is analysed. The solution is given for the diffracted field generated by incidence of a plane time-harmonic wave on a semi-infinite crack located in a plane normal to the axis of symmetry of the material. The exact solution is obtained by Fourier integral methods and the Wiener-Hopf technique. The method of solution applies when the slowness surfaces of the quasi-longitudinal and quasi-transverse waves are convex in the direction of the crack. The diffraction coefficients have been determined for regions of slowness-surface convexity. The diffraction coefficients have been used in the context of the geometrical theory of diffraction to compute high-frequency scattering by a crack of finite length. Applications to scattering by delaminations in a medium of periodic layering have been considered for the case when the wavelength and the crack length are of the same order of magnitude, but both are much larger than the larger layer thickness.

### 1. Introduction

THE propagation of waves in unbounded, homogeneous but anisotropic linearly elastic solids is well understood. The number of known solutions for scattering problems in anisotropic solids is, however, much smaller than for isotropic elasticity. The simplest problems, reflection and refraction of plane waves, have been discussed in detail (see for example (1, 2)). Lamb's problem for an anisotropic half-space was solved by Abubakar (3, 4) and Kraut (5).

In this paper we consider the problem of diffraction from a crack edge in an anisotropic solid. A semi-infinite crack is located in a plane of symmetry of a transversely isotropic material. The incident wave motion is confined to the plane which is normal to the crack edge. Therefore, the scattering geometry is two dimensional. A related problem of wave motion generated by symmetric concentrated forces on the crack faces in a material of cubic isotropy was considered in (6).

The two-dimensional isotropic diffraction problem was first solved by Maue (7). The three-dimensional isotropic problem was considered in (8, 9). The current problem can be viewed as a canonical problem whose solution is necessary for the development of an anisotropic geometrical theory of diffraction (GTD), see (9) for the isotropic theory.

After a brief review of wave propagation in a transversely isotropic solid in section 2, the diffraction problem is formulated in section 3. The Wiener-Hopf technique is used to obtain the solution. In section 4 we derive diffraction coefficients which permit us to extend GTD to include anisotropic diffraction. Finally in section 5 we consider a transversely isotropic solid as a model of a layered composite (each of the layers being isotropic), when the ratio of wave length and layer thickness is large. The crack is taken to be parallel to the layers. The diffracted field is compared to that of an isotropic solid and the implications for non-destructive testing of materials are noted.

## 2. Reflection of plane waves

As a preliminary to the discussion of diffraction by a semi-infinite crack, we give a brief review of the propagation of plane waves in transversely isotropic solids, and the reflection of plane waves at a traction-free boundary. The geometry is shown in Fig. 1. The y-axis is parallel to the axis of symmetry of the solid. The term  $\exp(-i\omega t)$  will be omitted.

For plane strain the stress-strain relations may be expressed in the form

$$\sigma_{\mathbf{x}} = \rho \{ a u_{\mathbf{x}} + (c - d) v_{\mathbf{y}} \}, \tag{2.1}$$

$$\sigma_{v} = \rho\{(c-d)u_{x} + bv_{y}\},\tag{2.2}$$

$$\sigma_{xy} = \rho d(u_y + v_x), \tag{2.3}$$

where  $u_x = \partial u/\partial x$ , etc., and

$$a = C_{11}/\rho, \qquad b = C_{33}/\rho,$$
 (2.4)

$$c = (C_{13} + C_{44})/\rho, \qquad d = C_{44}/\rho.$$
 (2.5)

Here  $C_{11}$ ,  $C_{13}$ ,  $C_{33}$  and  $C_{44}$  are four of the five elastic constants that enter in the three-dimensional stress-strain relations of a transversely isotropic solid. It is noted that for cubic isotropy we have  $a \equiv b$ , while the equations reduce

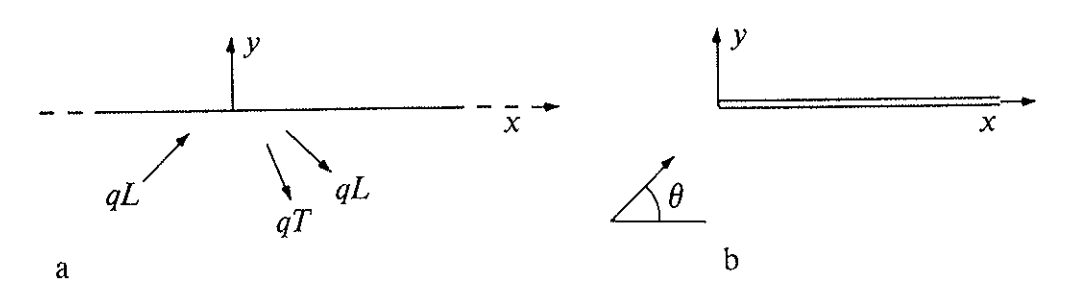


Fig. 1. Geometries for (a) reflection and (b) diffraction

to those for an isotropic solid when  $a \equiv b$  and c = a - d (then  $\rho a = \lambda + 2\mu$ ,  $\rho c = \lambda + \mu$  and  $\rho d = \mu$ ). By the use of (2.1) to (2.3) the displacement equations of motion are obtained as

$$au_{xx} + du_{yy} + cv_{xy} = -\omega^2 u, \qquad (2.6)$$

$$cu_{xy} + dv_{xx} + bv_{yy} = -\omega^2 v. \tag{2.7}$$

Let us first consider plane waves of the general form

$$\mathbf{u} = \{A_n(\lambda), B_n(\lambda)\} \exp\left[i\omega(\lambda x + \beta_n y)\right]. \tag{2.8}$$

Substitution of (2.8) into (2.6) to (2.7) gives

$$\begin{pmatrix} a\lambda^2 + d\beta_n^2 - 1 & c\lambda\beta_n \\ c\lambda\beta_n & d\lambda^2 + b\beta_n^2 - 1 \end{pmatrix} \begin{pmatrix} A_n \\ B_n \end{pmatrix} = \begin{pmatrix} 0 \\ 0 \end{pmatrix}.$$
 (2.9)

Let  $G(\lambda, \beta)$  be the determinant of the matrix in (2.9). The vanishing of this determinant defines the slowness surfaces,  $\beta = \pm \beta_n(\lambda)$ , n = 1, 2 where n defines the type of wave, and

$$\beta_n^2 = \frac{b + d - L\lambda^2}{2bd} + (-1)^n \left\{ \left( \frac{b + d - L\lambda^2}{2bd} \right)^2 - \frac{a}{b} \mu_1^2 \mu_2^2 \right\}^{\frac{1}{2}}.$$
 (2.10)

In (2.10),

$$L = ab + d^2 - c^2, (2.11)$$

$$\mu_n^2 = p_n^2 - \lambda^2;$$
  $p_1^2 = 1/a, p_2^2 = 1/d.$  (2.12)

In the isotropic limit, n=1 and n=2 correspond to longitudinal and transverse plane waves respectively. Therefore we refer to them in the anisotropic case as quasi-longitudinal and quasi-transverse waves.

The functions  $\beta_1(\lambda)$  and  $\beta_2(\lambda)$  possess several branch points in the complex  $\lambda$ -plane. These branch points are of two kinds. The first kind are those points at which  $\beta_1(\lambda)$  or  $\beta_2(\lambda)$  is zero. Assuming that a-d>0, which is the case in practice, we have that

$$\beta_1^2(p_1) = 0, \qquad \beta_2^2(p_1) > 0.$$
 (2.13)

Thus the points  $\lambda = \pm p_1$  are branch points of  $\beta_1(\lambda)$ . Now, if

$$c^2 < b(a-d),$$
 (2.14)

then we have

$$\beta_1^2(p_2) < 0, \qquad \beta_2^2(p_2) = 0,$$
 (2.15)

and so the points  $\lambda = \pm p_2$  are branch points of  $\beta_2(\lambda)$ . However, if

$$c^2 > b(a-d),$$
 (2.16)

then

$$\beta_1^2(p_2) = 0, \qquad \beta_2^2(p_2) > 0.$$
 (2.17)

· Condition (2.14) is equivalent to the condition that the quasi-transverse

slowness surface be convex in the x-direction (2, p. 103). In other words, if (2.16) holds, then the slowness surface is concave in the x-direction and the wave surface has two cusp points located symmetrically with respect to the x-axis (points  $Q_{II}$  in the notation of 2). The implication of (2.17) is that  $\beta_1(\lambda)$  has four branch points on the real axis and  $\beta_2(\lambda)$  has none. The real slowness surface  $(\lambda, \beta_2(\lambda))$  is therefore not closed, it is 'missing' those pieces where the quasi-transverse slowness surface is concave. These missing pieces are contained in  $\beta_1(\lambda)$ .

The second kind of branch points are where the discriminant of  $\beta_n^2(\lambda)$  is zero, that is where  $\beta_1^2(\lambda) - \beta_2^2(\lambda)$  is zero. Such points will occur in pairs. Between the two points of a given pair we may define a branch cut such that  $\beta_1(\lambda) + \beta_2(\lambda)$  is continuous across the cut while  $\beta_1(\lambda)$  and  $\beta_2(\lambda)$  are each discontinuous. In the analysis of the Appendix it turns out that  $\beta_1$  and  $\beta_2$  occur only in the combination  $\beta_1 + \beta_2$ . Therefore these cuts give no contribution to the analytic factorization in the Appendix.

The angle of incidence is defined as the angle that the ray direction of the incident plane wave makes with the positive x-axis. It follows from the definition of the ray direction (2) that the angle of incidence is the angle which the normal to the slowness surface makes with the x-axis. Let  $\theta_n$  be the angle of incidence of a wave of type n, then

$$\left. \frac{G_{\beta}}{G_{\lambda}} \right|_{\beta = \beta_{n}(\lambda)} = \tan \theta_{n}. \tag{2.18}$$

Thus, given n and  $\theta_n$ , equations (2.10) and (2.18) define the corresponding values of  $\lambda$  and  $\beta_n$ . Having found  $\lambda$  and  $\beta_n$  the corresponding ratio of  $B_n$  to  $A_n$  follows from (2.9) as

$$B_n/A_n = M_n(\lambda)/c\lambda\beta_n, \qquad (2.19)$$

where

$$M_n(\lambda) = -a\lambda^2 - d\beta_n^2 + 1. \tag{2.20}$$

To investigate the reflection of a plane wave of type n, n = 1, 2, we consider

$$\mathbf{u}^{\text{in}} = E_n \{ c\lambda \beta_n, M_n \} \exp \left[ i\omega (\lambda x + \beta_n y) \right], \tag{2.21}$$

where

$$E_n^{-2} = (c\lambda \beta_n)^2 + (M_n)^2. \tag{2.22}$$

The corresponding stresses at y = 0 are  $(\sigma_y^0, \sigma_{yx}^0) \exp(i\omega\lambda x)$ , where

$$\sigma_{y}^{0} = i\omega \rho E_{n} \beta_{n} G_{n}, \qquad (2.23)$$

$$\sigma_{yx}^0 = i\omega \rho E_n \beta_n F_n, \qquad (2.24)$$

and where

$$G_n = c(c-d)\lambda^2 + bM_n, \qquad (2.25)$$

$$F_n = (d\lambda/\beta_n)(c\beta_n^2 + M_n). \tag{2.26}$$

An incident wave of type n will give rise to reflection of waves of both types 1 and 2. A convenient form of the reflected wave field is:

$$\mathbf{u}^{\mathrm{re}} = R_1^n E_1 \{ c\lambda \beta_1, -M_1 \} \exp \left[ i\omega (\lambda x - \beta_1 y) \right] +$$

$$+R_2^n E_2 \{-c\lambda\beta_2, M_2\} \exp\left[i\omega(\lambda x - \beta_2 y)\right], \quad (2.27)$$

where  $R_1^n$  and  $R_2^n$  are the reflection coefficients. The conditions of vanishing stresses  $\sigma_y$  and  $\sigma_{yx}$  at y = 0 then gives the equations

$$\begin{pmatrix} G_1 & -G_2 \\ -F_1 & F_2 \end{pmatrix} \begin{pmatrix} E_1 \beta_1 R_1^n \\ E_2 \beta_2 R_2^n \end{pmatrix} = T E_n \beta_n \begin{pmatrix} G_n \\ F_n \end{pmatrix}. \tag{2.28}$$

This system of equations can be solved for  $R_1^n$  and  $R_2^n$  to yield

$$R_{m}^{n} = \frac{E_{n}\beta_{n}}{E_{m}\beta_{m}} \frac{F_{n}G_{3-m} + G_{n}F_{3-m}}{F_{1}G_{2} - F_{2}G_{1}},$$
(2.29)

where n defines the incident wave (n = 1, 2) and m the reflected wave (m = 1, 2).

# 3. Diffraction by a semi-infinite crack

The total field is expressed as the sum of the incident and the diffracted fields

$$\mathbf{u}^{\text{tot}} = \mathbf{u}^{\text{in}} + \mathbf{u},\tag{3.1}$$

where  $\mathbf{u}^{\text{in}}$  is given by (2.16) and  $\mathbf{u}$  represents the diffracted field. In the following we denote by  $\lambda_i$  the fixed value of  $\lambda$  for the incident wave.

The stress components of the diffracted field are denoted by  $\sigma_x$ ,  $\sigma_y$  and  $\sigma_{yx}$ . Since the total tractions must vanish on the faces of the crack, we have, for y = 0,  $x \ge 0$ , that

$$\sigma_{y} = -\sigma_{y}^{0} \exp(i\omega\lambda_{i}x), \tag{3.2}$$

$$\sigma_{yx} = -\sigma_{yx}^{0} \exp(i\omega\lambda_{i}x), \qquad (3.3)$$

where  $\sigma_y^0$  and  $\sigma_{yx}^0$  are given by (2.23) and (2.24). The plane of the crack is perpendicular to the axis of the transversely isotropic material, and hence (3.2) and (3.3) will give rise to displacement fields that are symmetric and antisymmetric respectively, with respect to the plane y=0. It is then convenient to formulate symmetric and antisymmetric problems separately for the half-plane  $y \ge 0$ . These are as follows.

Symmetric problem:

$$\sigma_{yx} = 0, \quad y = 0, -\infty < x < \infty,$$
 (3.4)

$$v = 0, \quad -\infty < x \le 0, \tag{3.5}$$

$$\sigma_{y} = -\sigma_{y}^{0} \exp(i\omega\lambda_{i}x), \qquad 0 < x < \infty.$$
 (3.6)

Antisymmetric problem:

$$\sigma_{y} = 0, \quad y = 0, -\infty < x < \infty,$$
 (3.7)

$$u = 0, \quad -\infty < x \le 0, \tag{3.8}$$

$$\sigma_{yx} = -\sigma_{yx}^{0} \exp(i\omega\lambda_{i}x), \qquad 0 < x < \infty. \tag{3.9}$$

We shall seek solutions to the problems formulated by (3.4) to (3.6) and (3.7) to (3.9) as superpositions of plane waves of types 1 and 2:

$$u = \sum_{m=1}^{2} \int_{-\infty}^{\infty} A_m(\lambda) e^{i\omega(\lambda x + \beta_m y)} d\lambda, \qquad (3.10)$$

$$v = \sum_{m=1}^{2} \int_{-\infty}^{\infty} \frac{M_m(\lambda)}{c\lambda \beta_m} A_m(\lambda) e^{i\omega(\lambda x + \beta_m y)} d\lambda.$$
 (3.11)

Also  $M_m$ , which is defined by (2.20), may be rewritten as

$$M_{\rm m} = -d\beta_{\rm m}^2 + a\mu_{\rm 1}^2. \tag{3.12}$$

Note that

$$\beta_1^2 + \beta_2^2 = (b + d - L\lambda^2)/bd;$$
  $\beta_1^2 \beta_2^2 = a\mu_1^2 \mu_2^2/b.$  (3.13)

The expressions for the stresses corresponding to (3.10) and (3.11) are

$$\sigma_{y} = \sum_{m=1}^{2} i\rho\omega \int_{-\infty}^{\infty} \left[ (c-d)\lambda + bM_{m}/c\lambda \right] A_{m}(\lambda) \exp\left[ i\omega(\lambda x + \beta_{m}y) \right] d\lambda, \quad (3.14)$$

$$\sigma_{yx} = \sum_{m=1}^{2} i\rho\omega \int_{\infty}^{\infty} d[\beta_m + M_m/c\beta_m] A_m(\lambda) \exp[i\omega(\lambda x + \beta_m y)] d\lambda. \quad (3.15)$$

Now for the symmetric problem the condition that  $v \equiv 0$  for y = 0,  $x \leq 0$ , implies that v(x, 0) may be expressed as

$$v(x,0) = \int_{-\infty}^{\infty} V^{-}(\lambda) \exp(i\omega\lambda x) d\lambda, \qquad (3.16)$$

where  $V^-(\lambda)$  is analytic in the lower half of the  $\lambda$ -plane. The condition that  $\sigma_{yx} = 0$  at y = 0 and the use of (3.15) and (3.11) yields expressions for  $A_2(\lambda)$  and  $A_1(\lambda)$  in terms of  $V^-(\lambda)$ . The application of these expressions in (3.14) subsequently gives

$$\sigma_{y}(x,0) = i\rho\omega \int_{-\infty}^{\infty} \frac{R(\lambda)}{\mu_{1}(\lambda)} V^{-}(\lambda) e^{i\omega\lambda x} d\lambda, \qquad (3.17)$$

where

$$R(\lambda) = \frac{\mu_2(F_1G_2 - F_2G_1)}{acd\lambda(\beta_1^2 - \beta_2^2)}.$$
 (3.18)

We may also write

$$\sigma_{y}(x,0) = \int_{-\infty}^{\infty} \left[ T^{+}(\lambda) + T^{-}(\lambda) \right] e^{i\omega\lambda x} d\lambda, \qquad (3.19)$$

where  $T^+$  and  $T^-$  are analytic in the upper and lower halves of the  $\lambda$ -plane respectively. It follows from (3.6) that

$$T^{-}(\lambda) = \frac{i\sigma_{y}^{0}}{2\pi\rho\omega(\lambda - \lambda_{i})}.$$
 (3.20)

By equating (3.17) and (3.19) we obtain

$$i\frac{R(\lambda)}{\mu_1(\lambda)}V^{-}(\lambda) = T^{+}(\lambda) + T^{-}(\lambda). \tag{3.21}$$

Equation (3.21) is of the type that can be solved by the Wiener-Hopf technique. Here we state briefly the formal procedure and the result. For details we refer to the Appendix. First we introduce the auxiliary function

$$K(\lambda) = ZR(\lambda)/(\lambda^2 - \lambda_R^2), \tag{3.22}$$

where  $\lambda = \pm \lambda_R$  are the roots of  $R(\lambda) = 0$ , and Z is a constant which is chosen such that  $K(\lambda) \to 1$  as  $|\lambda| \to \infty$ . In the complex  $\lambda$ -plane,  $K(\lambda)$  may be factored in the standard manner (see the Appendix) as

$$K(\lambda) = K^{+}(\lambda)K^{-}(\lambda), \tag{3.23}$$

where  $K^+(\lambda)$  and  $K^-(\lambda)$  are analytic in the upper and lower halves of the  $\lambda$ -plane respectively. The following relation holds:

$$K^{-}(\lambda) = K^{+}(-\lambda). \tag{3.24}$$

To solve (3.21) it is rewritten as

$$\frac{(T^{-} + T^{+})\mu_{1}^{+}(\lambda)}{(\lambda + \lambda_{R})K^{+}(\lambda)} = \frac{i(\lambda - \lambda_{R})K^{-}(\lambda)V^{-}}{Z\mu_{1}^{-}(\lambda)},$$
(3.25)

where  $\mu_1^{\pm}(\lambda)$  follow from (2.12):

$$\mu_1^{\pm} = (p_1 \pm \lambda)^{\frac{1}{2}} \tag{3.26}$$

The right-hand side of (3.25) is analytic in the lower half of the  $\lambda$ -plane. On the left-hand side, the term  $T^-$ , which is given by (3.20), contains a pole at  $\lambda = \lambda_i$ . Now we subtract the term

$$T^{-}\mu_{1}^{+}(\lambda_{i})/(\lambda_{R} + \lambda_{i})K^{+}(\lambda_{i})$$
(3.27)

from both sides of (3.25), to obtain an equation whose right-hand side and left-hand side are analytic in the lower and the upper half of the  $\lambda$ -plane respectively. By the usual Wiener-Hopf argument the right-hand side and the left-hand side must then be equal to the same entire function. We note

that the Wiener-Hopf technique requires the left- and right-hand sides to be analytic in a common strip. Such a strip may be obtained by giving  $p_1$  and  $p_2$  small imaginary parts. This mathematical device is physically equivalent to introducing dissipation. The loss-less case is then found by letting the strip collapse onto the real axis.

In the plane of the crack (y=0) and near the crack edge we have  $v \sim x^{\frac{1}{2}}$ . It is known that  $v \sim x^{\frac{1}{2}}$  implies  $V^- \sim \lambda^{-\frac{3}{2}}$  as  $|\lambda| \to \infty$ . By virtue of this observation the entire function represented by the left-hand side of (3.25) minus the term given by (3.27) must then be identically zero, which leads to the result that

$$V^{-}(\lambda) = \frac{\sigma_{y}^{0}Z}{2\pi\rho\omega} \frac{\mu_{1}^{-}(\lambda)\mu_{1}^{+}(\lambda_{i})}{(\lambda_{i} + \lambda_{R})(\lambda - \lambda_{R})K^{-}(\lambda)K^{+}(\lambda_{i})(\lambda - \lambda_{i})}.$$
 (3.28)

The antisymmetric problem may be solved by first writing u(x, 0) as

$$u(x,0) = \int_{-\infty}^{\infty} U^{-}(\lambda)e^{i\omega\lambda x} d\lambda, \qquad (3.29)$$

where  $U^{-}(\lambda)$  is analytic in the lower half plane. This representation of u(x,0) satisfies the condition that  $u\equiv 0$  for y=0,  $x\leq 0$ . The remainder of the analysis is completely analogous to that for the symmetric problem. We just cite the result that

$$U^{-}(\lambda) = \frac{\sigma_{yx}^{0}Z}{2\pi\rho\omega} \frac{\mu_{2}^{-}(\lambda)\mu_{2}^{+}(\lambda_{i})}{(\lambda_{i} + \lambda_{R})(\lambda - \lambda_{R})K^{-}(\lambda)K^{+}(\lambda_{i})(\lambda - \lambda_{i})}.$$
 (3.30)

The solution for **u** to the full problem may be expressed as in (3.10) and (3.11) where  $A_1(\lambda)$  and  $A_2(\lambda)$  are now

$$A_1(\lambda) = \frac{a\mu_1 G_2 U^- - b\mu_2 F_2 V^-}{abd\mu_1 (\beta_1^2 - \beta_2^2)},$$
(3.31)

$$A_2(\lambda) = \frac{-a\mu_1 G_1 U^- + b\mu_2 F_1 V^-}{abd\mu_1 (\beta_1^2 - \beta_2^2)}.$$
 (3.32)

# 4. Asymptotic diffracted field

We now discuss the form of the scattered field given by (3.10) and (3.11) at a large radial distance from the crack tip. The general type of integral to be considered is

$$I_{m} = \int_{-\infty}^{\infty} F(\lambda) \exp\left[i\omega r(\lambda \cos \theta + \beta_{m} \sin \theta)\right] d\lambda, \tag{4.1}$$

where m = 1, 2, and  $(r, \theta)$  are polar coordinates defined by

$$x = r \cos \theta, \qquad y = r \sin \theta.$$
 (4.2)

For large r this integral can be approximated by deforming the path of

integration to a contour of steepest descent through the point of stationary phase. In deforming to the steepest-descent contour certain poles and branch cuts may be encountered in the complex  $\lambda$ -plane. The first pole is at  $\lambda = \lambda_R$ , which corresponds to the surface waves on the crack faces. The other pole is at  $\lambda = \lambda_i$  which gives rise to specular reflection and the shadow zone. The branch-cut contributions are exactly analogous to the phenomenon of head waves in isotropic diffraction theory. Since each of these features has been well discussed for isotropic diffraction, we shall concentrate our attention on the steepest-descent contribution.

The point of stationary phase occurs at  $\lambda_0$  such that

$$\left. \frac{G_{\beta}}{G_{\lambda}} \right|_{\beta = \beta_{m}(\lambda_{0})} = \tan \theta. \tag{4.3}$$

At this stage we make the additional assumption that the slowness surface of type m is convex at  $\lambda_0$ . The method of stationary phase then gives (10)

$$I_{m} \sim e^{-i\pi/4} \left| \sin \theta \right| \left( \frac{2\pi\gamma_{0}}{\omega_{r}} \right)^{\frac{1}{2}} F(\lambda_{0}) \exp \left[ i\omega r(\lambda_{0} \cos \theta + \beta_{m}(\lambda_{0}) \left| \sin \theta \right|) \right], \quad (4.4)$$

where  $\gamma_0$  is the curvature of the slowness surface at  $\lambda_0$ :

$$\gamma_0 = |G_{\lambda}^2 G_{\beta\beta} + G_{\beta}^2 G_{\lambda\lambda} - 2G_{\lambda} G_{\beta} G_{\lambda\beta}| (G_{\lambda}^2 + G_{\beta}^2)^{-\frac{3}{2}}|_{\beta = \beta_{m}(\lambda_0)}. \tag{4.5}$$

We note that the convexity condition is always satisfied for the quasi-longitudinal wave (2). However, the quasi-transverse slowness surface may have concave regions. If  $\lambda_0$  is in such a region the above asymptotic approximation becomes invalid; we refer to (11) for more details.

Combining the above result with (3.10) and (3.11) we obtain the far-field of type m due to an incident wave of type n:

$$\mathbf{u}^{m} \sim \frac{1}{(p_{2}\omega r)^{\frac{1}{2}}} E_{m}(c\lambda\beta_{m}, M_{m})|_{\lambda = \lambda_{0}} D_{m}^{n}(\theta; \theta_{n}) \exp\left[i\omega r(\lambda_{0}\cos\theta + \beta_{m}(\lambda_{0})|\sin\theta|)\right]. \tag{4.6}$$

In this expression the unit displacement vector see (2.21) is divided by the square root of the non-dimensional distance  $p_2\omega r$ , where  $p_2$  is defined in (2.12). The quantity  $D_m^n$  is the diffraction coefficient:

$$D_{m}^{n}(\theta;\theta_{n}) = (-1)^{3-m} e^{i\pi/4} \left(\frac{p_{2}\gamma_{0}}{2\pi}\right)^{\frac{1}{2}} \frac{Z}{abcd} \frac{E_{n}\beta_{n}}{E_{m}\beta_{m}} \mu_{2}(\lambda_{0}) \times \\ \times \frac{\left[\sin\theta a F_{n} G_{3-m} \mu_{2}^{+}(\lambda_{i})/\mu_{2}^{+}(\lambda_{0}) - |\sin\theta| b G_{n} F_{3-m} \mu_{1}^{+}(\lambda_{i})/\mu_{1}^{+}(\lambda_{0})\right]}{\lambda_{0} \left[\beta_{1}^{2}(\lambda_{0}) - \beta_{2}^{2}(\lambda_{0})\right] (\lambda_{0} - \lambda_{i})(\lambda_{0} - \lambda_{R})(\lambda_{i} + \lambda_{R}) K^{+}(\lambda_{i}) K^{+}(-\lambda_{0})},$$
(4.7)

where the quantities with subscripts n and m are evaluated at  $\lambda_i$  and  $\lambda_0$  respectively. It can be shown that these diffraction coefficients reduce to those of isotropic elasticity (9) in the appropriate limit. The far-field of (4.6) is singular at the physical elastodynamics reflection and shadow boundaries. This is attributable to the inadequacy of the asymptotic expansion (4.4) at these boundaries. The singularities may be removed using a uniform asymptotic analysis of the integrals  $I_m$ : see for example (9).

## 5. Examples for a layered medium

In this section we consider a laminated composite consisting of alternating plane parallel layers of two homogeneous, isotropic, elastic materials with the same density. The exact dynamic theory of such a medium presents many difficulties particularly if one should want to consider simultaneously the effects of the layered structure and a crack edge. However, a useful approach is to use an effective modulus theory (12) whereby the laminated medium is approximated by an equivalent anisotropic but homogeneous elastic material. Although this is a static theory, it may be used for dynamic problems when the typical wavelength is much larger than the larger of the two layer thicknesses.

According to effective modulus theory (12), the gross elastic behaviour of the laminated medium is transversely isotropic with the normal to the layers as the axis of symmetry. The effective elastic constants  $C_{11}$ ,  $C_{33}$ ,  $C_{13}$  and  $C_{44}$  are given in (12, p. 33).

For the examples of this section we consider the case when the elastic materials of both layers have a Poisson's ratio of  $\frac{1}{3}$ , which corresponds to a bulk-wave-speed ratio of 2. Let the x-axis be in the direction of the layers and the y-axis be normal to the layers. Then the effective elastic constants are

$$C_{11} = \left[4(l+\bar{l})^{2}\mu\bar{\mu} + 3l\bar{l}(\mu - \bar{\mu})^{2}\right]/\left[(l\bar{\mu} + l\bar{\mu})(l+\bar{l})\right],$$

$$C_{33} = 4C_{44}, \qquad C_{13} = 2C_{44},$$

$$C_{44} = (l+\bar{l})\mu\bar{\mu}/(l\bar{\mu} + \bar{l}\mu),$$
(5.1)

where l,  $\bar{l}$  are the thicknesses and  $\mu$ ,  $\bar{\mu}$  the shear moduli of the two elastic layers. The parameters a, b, c and d follow from (2.4) and (2.5). Since it is only the relative magnitue of these constants that is of importance we need only the ratios

$$a/d = 4 + 3\varepsilon (1 - \varepsilon) [1/(\alpha - \alpha^2) - 4],$$

$$b/d = 4, \qquad c/d = 3,$$
(5.2)

where we have defined  $0 \le \alpha \le 1$  and  $0 \le \epsilon \le 1$  as

$$\alpha = \mu/(\mu + \bar{\mu}),\tag{5.3}$$

$$\varepsilon = l/(l + \overline{l}). \tag{5.4}$$

We note that  $a/d \ge 4$ , with equality only in the trivial limit when the composite is homogeneous. Thus  $(a/b)^{\frac{1}{2}}$ , which is the ratio of the longitudinal wave speed parallel to the layers to that normal to the layers, is greater than unity.

We now consider a semi-infinite crack parallel to the layers in the composite medium. The solution to the diffraction problem is obtained using the effective medium hypothesis. The elastic constants of (5.2) automatically satisfy the condition that the quasi-transverse slowness surface be convex in the direction of the crack, see the Appendix. Convexity in the y-direction is also ensured by (5.2) (see (2, (8.3.4))). We note in connection with the Appendix and (2.11), that L>0.

The quasi-longitudinal slowness surface is always convex in transverse isotropy. The same is not true of the quasi-transverse slowness surface. Musgrave and Payton (13) have derived a simple condition which is sufficient and slightly more than necessary for the existence of inflexion points on the slowness surface away from the symmetry axes. It is

$$c + 2d + [(a-d)(b-d)]^{\frac{1}{2}} < 2(a-d)(b-d)/c.$$
 (5.5)

This condition is met by the parameters of (5.2) if

$$a/d > \frac{1}{8}(31 + \sqrt{129}) \approx 5.3.$$

Thus, when the ratio of the longitudinal speeds normal and parallel to the layers exceeds 1.15, cusps will appear in the quasi-transverse wave surface (2). The far-field solution of (4.6) with n or m equal to 2 then becomes invalid in certain angular sectors (11).

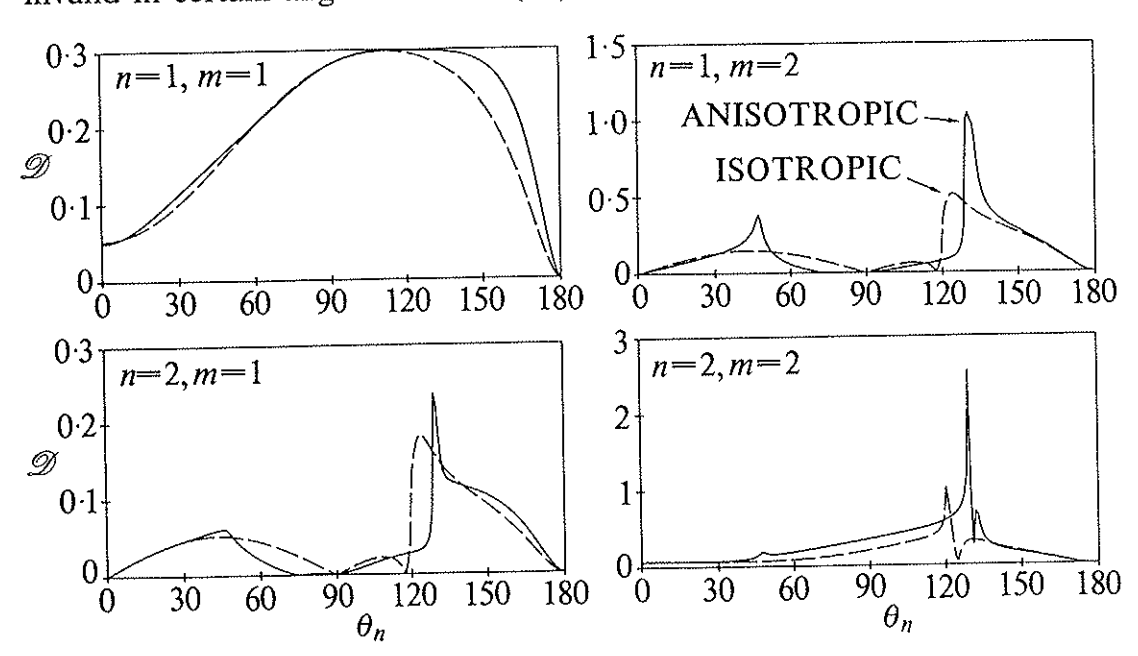


Fig. 2. Graphs of  $\mathcal{D} = |\cos \theta_n D_m^n(\theta_n + \pi, \theta_n)|$  for a/d = 5. The  $\cos \theta_n$ -term is included to remove the reflection singularities of  $D_1^1$  and  $D_2^2$  at  $\theta_n = \frac{1}{2}\pi$ 

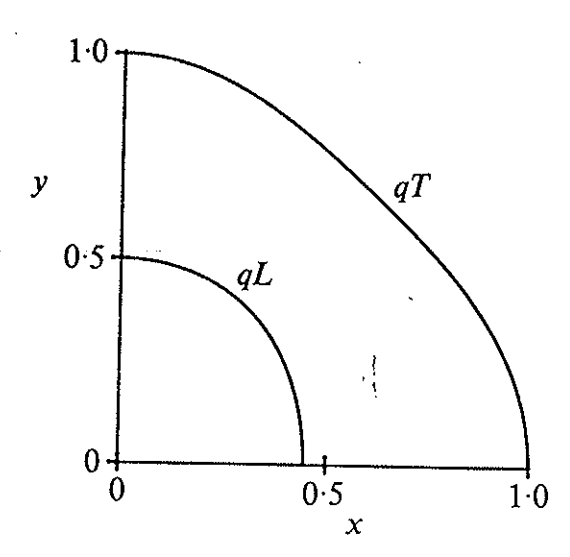


Fig. 3. Sections of the slowness surfaces for a/d = 5

The four diffraction coefficients of (4.7) have been plotted as functions of angle  $\theta$  in Fig. 2 for a/d=5 and  $\theta=\pi+\theta_n$ , which corresponds to observation from the direction of incidence (pulse echo), see Fig. 1. The isotropic coefficient with a/d=4 are shown for comparison. The corresponding slowness surfaces are shown in Fig. 3. When a/d=10 the slowness surfaces are as shown in Fig. 4. For that case we have plotted only the diffraction coefficient  $D_1^1$  in Fig. 5.

Cracks in the direction of the layering (delaminations) occur frequently. According to the geometrical theory of diffraction, the diffraction coefficients for the semi-infinite crack can be used to compute the high-frequency scattered field for a crack of finite length D. Let a plane quasi-longitudinal wave of unit amplitude be incident on the crack at angle  $\theta$ . The diffracted

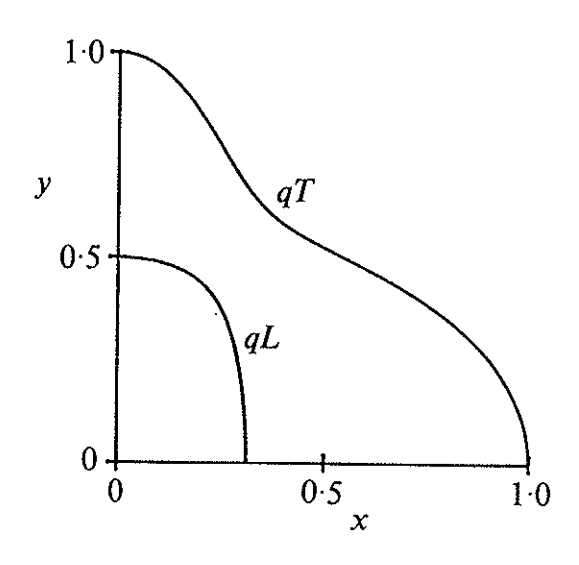


Fig. 4. Sections of the slowness surfaces for a/d = 10

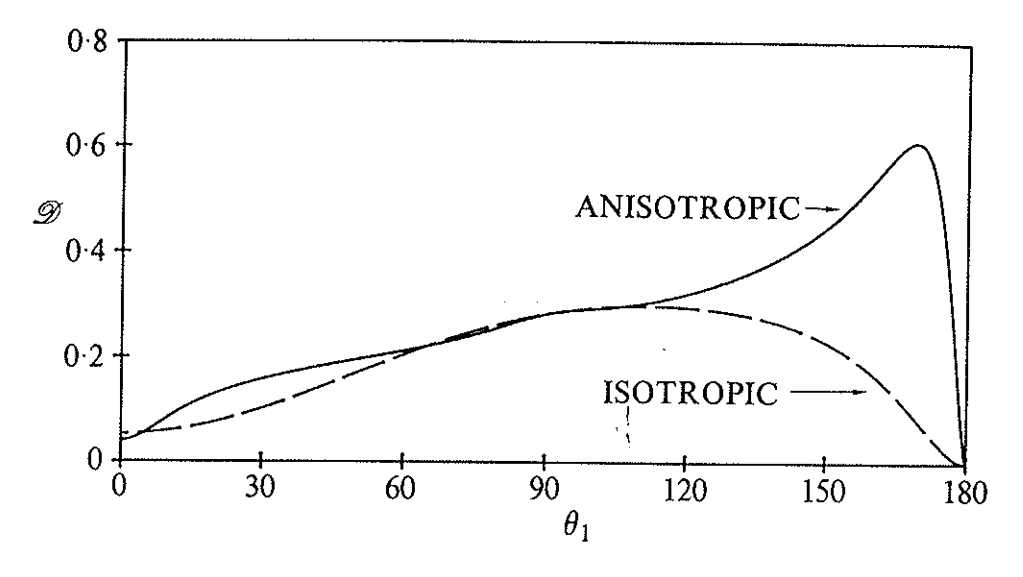


Fig. 5. Graph of  $\mathfrak{D} \equiv |\cos \theta_1 D_1^1(\theta_1 + \pi, \theta_1)|$  for a/d = 10

quasi-longitudinal field in the back scattered direction can then be computed by using (4.6) for each tip of the crack individually. Superposition of the two crack-tip diffractions gives a high-frequency approximation to the back scattered or pulse-echo signal. In this approximation all multiply diffracted rays are neglected. It is assumed that D is of the same order as the wavelength. Since the wavelength must be much larger than the layer thicknesses for the effective modulus theory to be valid, we must also require that D is much larger than the larger layer thickness.

Taking the origin at the centre of the crack, we have plotted the far field amplitude  $(r/D)^{\frac{1}{2}}|\mathbf{u}(r,\theta)|$  in Fig. 6 as a function of the dimensionless frequency  $D\omega/\sqrt{b}$ . We note that  $\omega/\sqrt{b}$  is the longitudinal wave number in the direction normal to the slit  $(\theta = \frac{1}{2}\pi)$ . The value of a/d in Fig. 6 is 10, corresponding, for example, to  $\varepsilon = \frac{1}{2}$  and  $\alpha = (1 + \sqrt{\frac{2}{3}})/2 \approx 0.91$  in (5.2). The isotropic result (a = b) is also plotted in Fig. 6 for comparison. Because b is the same for the two examples, the effect of anisotropy disappears at normal incidence.

The simple diffraction theory used here is only reasonable at high frequency and does not attempt to give the low-frequency scattering. The latter could be found, for example, from a quasi-static analysis. However, our results show that the anisotropy is important, especially at angles of incicence near grazing.

# Acknowledgment

The work reported here was carried out in the course of research under contract DE-AC02-83ER13036.A000, with the Department of Energy, Office of Basic Energy Sciences, Engineering Research Program.

J. 19

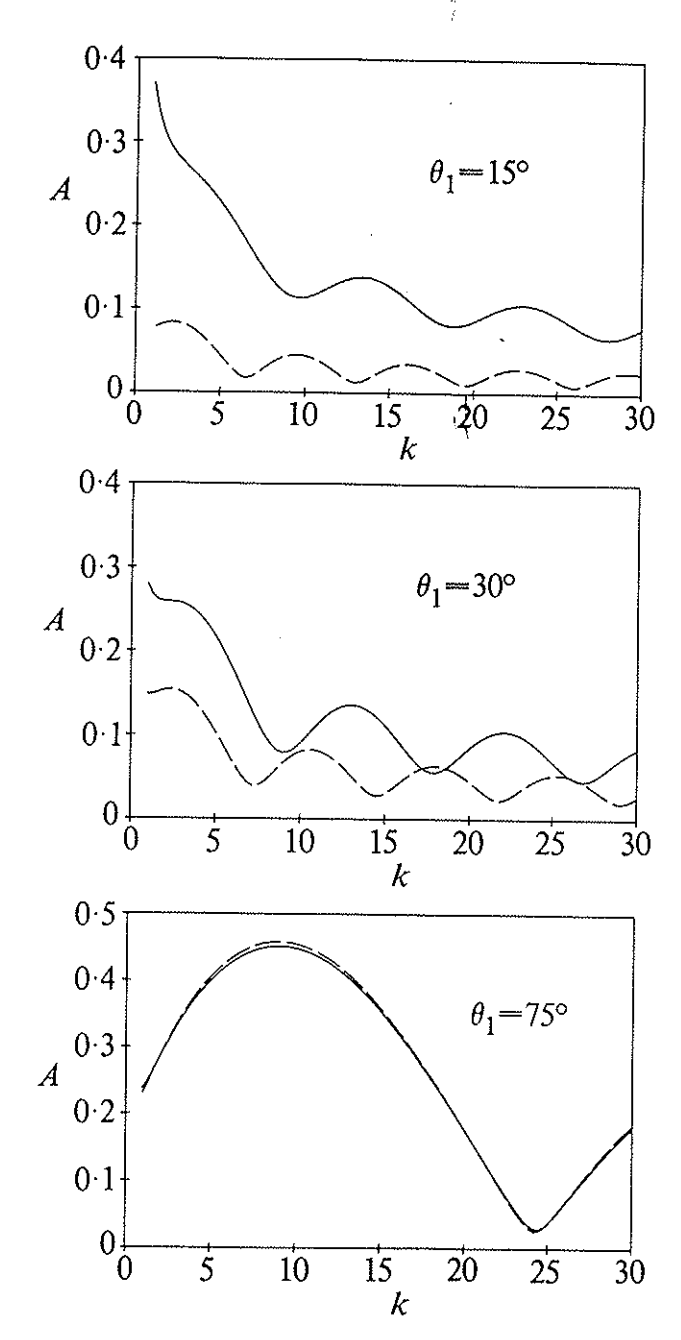


Fig. 6. Backscattered far-field quasi-longitudinal amplitude  $A = |\mathbf{u}| \sqrt{r/D}$  as a function of frequency  $k = \omega D/\sqrt{b}$  for a/d = 10

### REFERENCES

- 1. M. J. P. Musgrave, Geophys. J. R. Ast. Soc. 3, (1960) 406.
- 2. —, Crystal Acoustics (Holden Day, San Francisco, 1970).
- 3. I. ABUBAKAR, Geophys. J. 6 (1962) 337.
- **4.** —, *ibid.* **7** (1962) 87.
- 5. E. A. KRAUT, Rev. of Geophys. 1 (1963) 401.
- 6. A. N. MARTIROSIAN, Proc. Acad. Nauk Armenian SSR 28 (1975) 33 (Russian).
- 7. A. W. MAUE, Z. angew. Math. Mech. 33 (1953) 1.

- 8. J. D. Achenbach and A. K. Gautesen, J. Acoust. Soc. Am. 61 (1977) 413.
- 9. \_\_\_\_, \_\_\_ and H. McMaken, Ray Methods for Waves in Elastic Solids (Pitman, London, 1982).
- 10. M. J. LIGHTHILL, Phil. Trans. R. Soc. A 252 (1960) 397.
- 11. V. T. BUCHWALD, Proc. R. Soc. A 253 (1959) \$63.
- 12. J. D. ACHENBACH, A Theory of Elasticity with Microstructure for Directionally Reinforced Composites (Springer, Berlin, 1975).
- 13. M. J. P. MUSGRAVE and R. G. PAYTON, J. Elasticity, to appear.
- 14. J. D. Achenbach, Wave Propagation in Elastic Solids (North-Holland, Amsterdam, 1973).
- 15. R. STONELEY, Proc. R. Soc. A 232 (1955) 447.

### APPENDIX

Factorization of  $K(\lambda)$ 

In order to investigate the analytic nature of  $K(\lambda)$ , we first write it in the form

$$K(\lambda) = K_0(\lambda)K_1(\lambda), \tag{A.1}$$

where

$$K_0(\lambda) = \frac{-ad}{2(a-d)} \left[ \frac{4\lambda^2 \mu_1 \mu_2 + (\mu_2^2 - \lambda^2)^2 + P(\lambda^2 + \mu_1 \mu_2) + Q}{\lambda^2 - \lambda_R^2} \right], \tag{A.2}$$

$$K_1(\lambda) = -Z \frac{[ab - (c - d)^2] \mu_1 + \mu_2}{2a \beta_1 + \beta_2}$$
(A.3)

and

$$P = 4 \frac{(\sqrt{ab - b})}{ab - (c - d)^2},$$
(A.4)

$$Q = \frac{P}{\sqrt{ab}} + \frac{b(b-a) + (c+d-b)(c+b-3d)}{d^2 [ab - (c-d)^2]}.$$
 (A.5)

Both  $K_0(\lambda)$  and  $K_1(\lambda)$  tend to unity as  $|\lambda| \to \infty$ . This implies that

$$Z = \frac{-a}{(2bd)^{\frac{1}{2}}} \frac{\left[-L + (L^2 - 4abd^2)^{\frac{1}{2}}\right]^{\frac{1}{2}} + \left[-L - (L^2 - 4abd^2)^{\frac{1}{2}}\right]^{\frac{1}{2}}}{i\left[ab - (c - d)^2\right]},$$
 (A.6)

where L is given in (2.11) and the square root function is defined such that Im () $^{\frac{1}{2}} \ge 0$ . Thus Z is real if L > 0, which we shall assume in this paper.

The function  $K_0(\lambda)$  is similar in form to the Rayleigh function for an isotropic half-space. It essentially reduces to that function when P=Q=0. By application of the principle of the argument (14, p. 190) it can be shown that  $(\lambda^2-\lambda_R^2)K_0(\lambda)$  has only two zeros in the complex  $\lambda$ -plane, at  $\lambda=\pm\lambda_R$ . We note that  $K_0(\lambda)$  is real for  $\lambda$  real and greater than  $p_2$ , which is greater than  $p_1$ . At  $\lambda=p_2$ , the function  $(\lambda^2-\lambda_R^2)K_0(\lambda)$  is equal to  $-2(ab)^{\frac{1}{2}}/[ab-(c-d)^2]$ , while as  $\lambda\to\infty$ , it is approximately  $\lambda^2$ . Thus, if  $ab-(c-d)^2>0$ , as we shall presume, then  $\lambda_R$  is real and greater than  $p_2$ . The root  $\lambda=\lambda_R$  is the surface wave slowness on the crack faces. We note that L>0 is a necessary but not sufficient condition for the surface wave to decay exponentially with depth (15). The function  $K_0(\lambda)$  also has branch cuts between  $-p_2$  and  $-p_1$  and between  $p_1$  and  $p_2$ . Therefore it is completely analogous to the isotropic Rayleigh function, whose analytic factorization has been discussed, for example in (9, p. 141). Proceeding as in (9) we obtain

where

$$K_0^+(\lambda) = \exp\frac{-1}{\pi} \int_{p_1}^{p_2} \tan^{-1} \left\{ \frac{(4t^2 + P)(p_2^2 - t^2)^{\frac{1}{2}}(t^2 - p_1^2)^{\frac{1}{2}}}{(p_2^2 - 2t^2)^2 + Pt^2 + Q} \right\} \frac{dt}{t + \lambda} . \tag{A.8}$$

The function  $K_1(\lambda)$  has branch points at  $\pm p_1$  and  $\pm p_2$ , the branch points of  $\mu_1$  and  $\mu_2$ , respectively. In addition, there are branch points of the functions  $\beta_1(\lambda)$  and  $\beta_2(\lambda)$ . These branch points are of two kinds. The first kind are those points at which  $\beta_1(\lambda)$  and  $\beta_2(\lambda)$  are zero. In section 2 it was shown that these branch points of  $\beta_1(\lambda)$  and  $\beta_2(\lambda)$  coincide with the branch points of  $\mu_1(\lambda)$  and  $\mu_2(\lambda)$  respectively if and only if the quasi-transverse slowness surface is convex in the direction of the crack. The branch points at which the discriminant of  $\beta_n^2(\lambda)$  is zero do not affect the factorization since  $\beta_1$  and  $\beta_2$  occur only in the combination  $\beta_1 + \beta_2$ , which is continuous across these cuts (see section 2). Therefore, assuming that (2.14) is satisfied, the factorization of  $K_1(\lambda)$  proceeds in the same manner as for  $K_0(\lambda)$ . We obtain

$$K_1(\lambda) = K_1^+(\lambda) K_1^-(\lambda), \tag{A.9}$$

where

$$K_1^+(\lambda) = \exp\frac{-1}{\pi} \int_{p_1}^{p_2} \tan^{-1} \left\{ \frac{i(\mu_2 \beta_1 - \mu_1 \beta_2)}{\mu_2 \beta_2 - \mu_1 \beta_1} \right\} (t) \frac{dt}{t + \lambda} . \tag{A.10}$$

We note that  $\mu_1(t)$  and  $\beta_1(t)$  are imaginary for t between  $p_1$  and  $p_2$  while  $\mu_2(t)$  and  $\beta_2(t)$  are real.

The complete factorization of  $K(\lambda)$  is

$$K^{+}(\lambda) = K_0^{+}(\lambda)K_1^{+}(\lambda). \tag{A.11}$$

Finally, we note that

$$K(0) = [K^{+}(0)]^{2} = -\frac{b}{a} \frac{Z}{\lambda_{P}^{2}}.$$
 (A.12)

This relation provides a means of determining  $\lambda_R$  quite simply or may be used as a check on  $K^+(\lambda)$  if  $\lambda_R$  is known.